Article

Study on blast waves generated by milligram charges

Kentaro Ohashi[***], Harald Kleine[*], and Kazuyoshi Takayama[**]

The blast wave from the detonation of a cylindrical charge of silver azide with a charge mass varying between 10mg and 0.5mg is described based on experimental results of pressure measurements and visualizations. Primary shock wave, secondary shock wave, and detonation products are seen on sequences of photos taken with an image converter camera. From these pictures x-t diagrams could be established and based on these x-t data, the overpressure could be obtained as a function of distance. Comparing the obtained face-on overpressure data with TNT reference data against scaled distance, the blast waves generated by the investigated charges were seen to follow the cube-root scaling law. Furthermore an average TNT equivalence factor of silver azide was found to be approximately 0.45.

1. Introduction

The study of explosion phenomena is an important research field for safety assessment and for the analysis and prediction of explosion disasters. Blast waves are produced by the sudden release of energy from sources such as a chemical detonation, a nuclear explosion, or the rupture of a pressurized vessel. These waves are characterized by a supersonic shock front followed by an exponential-type decay of the physical properties of the gas [1]. Occasionally, some of the fragments of these sources may pass through and move ahead of the shock front.

In large-scale experiments, which have been intensively carried out over the last decades, many diagnostic techniques have been developed to measure the physical properties of a gas subjected

to a blast wave [1, 2]. In small-scale laboratory experiments, on the other hand, different diagnostics are available, which may be difficult to implement in large-scale tests. This concerns mainly density-sensitive flow visualization techniques such as shadowgraph, schlieren methods, and interferometry. These techniques allow us to visualize and quantify the full flow field including primary and secondary shock waves and the contact surface enveloping the cloud of combustion products [3]. Apart from significantly reduced cost, another major advantage of small-scale tests is the short turnover time between experiments – more than 30 trials per day can be performed without difficulty. The gathered information is useful for a thorough validation of computer codes for blast wave simulation, since the experimental and numerical results can easily be brought to the same format for comparison.

One of the main results of the numerous large-scale trials conducted throughout the last century is that many blast wave parameters can be scaled for charge masses varying from a few grams up to several tons [1, 2, 4]. In this study it was to be shown that the same scaling law could also be applied for much lower charge masses of the order of a few milligrams [5].

2. Experiment

Three sets of experiments were conducted, namely measurement of face-on overpressure, time-resolved schlieren visualization, and direct shadowgraph of the blast wave flow fields. From these records, the propagation of the generated blast waves could be mapped in corresponding x-t diagrams and an average TNT equivalence factor of the used explosive (silver azide) could be determined.

2.1 Explosive charges

The blast waves were generated by the detonation of silver azide pellets (AgN_3; charge density: 3.77g/cm³, manufactured by Chugoku-Kayaku Co. Ltd.) with masses of 0.5mg±5%, 1mg±1%, 5mg±1%, and 10mg±1%. The larger charges (mass of 10mg and 5mg) are cylindrical, while the shapes of smaller charges (masses of 1mg and 0.5mg) are irregular because these charges are obtained by removing material from larger ones.

2.2 Overpressure measurements

In the overpressure tests, the charge was glued to an optical fiber and ignited by the irradiation of a pulsed Nd:YAG laser (1064nm, 7ns pulse duration, 25mJ/pulse) fed through this fiber.
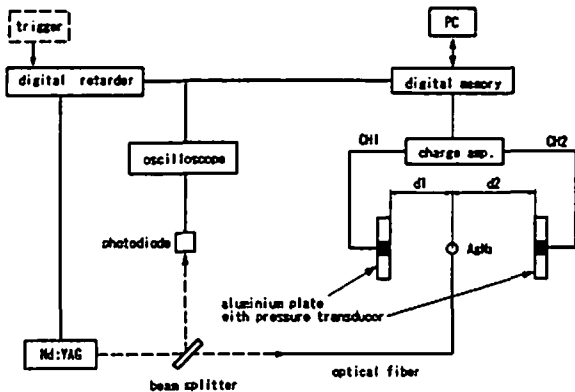
F i g . 1 Schematic of the overpressure measurement setup

Figure1 shows the schematic of the overpressure measurement setup. The charge was placed between two plates, each of which was equipped with one piezo-electric pressure transducer (Kistler603B, response time < 2μs, sensitive area:

9.1mm²). The pressure gauges and the charges were set to be on the same height. The transducers were facing each other and aligned on one axis with the charges. Distances between the center of the charge and the transducer (d_1, d_2 in Fig.1) ranged from 10 ± 0.1mm to 200 ± 0.1mm in steps of 10mm. For smaller distances, the size of the pressure transducer becomes too large with respect to the radius of the blast wave; for larger distances, the signal-to-noise ratio increases due to weak pressure signals; for distances larger than 200mm one also has to consider that the size of the plate is insufficient for recording the whole pressure history as corner signals may reach the transducer before the blast wave profile is completed [5, 6]. Pressure signals were recorded into a digital memory with a sampling rate of 2MHz. For each configuration three experiments were conducted, the total number of pressure measurements amounted to 200 trials.

In a set of preparatory experiments [6] the ignition threshold of silver azide had been found to be around 100μJ with an ignition delay of less than 1μs. The instant of ignition therefore corresponds with sufficient accuracy to the instant when the Nd:YAG laser is fired, which can be measured by means of a photodiode as indicated in Fig.1.

2.3 Density-sensitive flow visualization

In these tests, the charge was glued to a nylon thread and ignited by direct irradiation of the Nd:YAG laser. Visualization was performed using time-resolved monochrome schlieren shown schematically in Fig.2.
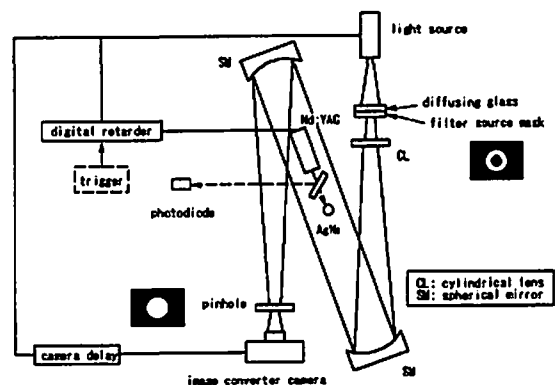
F i g . 2 Schematic of time-resolved schlieren method

Analogous to the configuration in a colour schlieren apparatus [7] a diffusing screen with a circular source mask was illuminated by a light source (a flashlamp that provided intense illumination for about 1ms), while a pinhole was used as cutoff device. This resulted in a system that was equally sensitive to gradients in all directions. A cylindrical lens in front of the source mask was required for astigmatic correction [7]. The images were recorded with an image converter camera which could take 6 frames per test with an individual exposure time set to 200ns. This system helps to interpret the explosion phenomena such as the propagation of blast waves, the generation of the cloud of detonation products, and also the fragmentation of explosives. In particular the propagation of the generated blast waves can be established from the time sequential photos obtained with this method. Furthermore the reflected overpressure can be determined as x-t data and overpressure are linked through the Rankine-Hugoniot relationships. Finally, the equivalence factor of silver azide can be determined by comparison with TNT reference data.

3. Analysis, results and discussions
3.1 Shock front properties

The arrival of the shock front leads to a pressure jump from atmospheric pressure P_1 to the shock-generated pressure P_2. The pressure increment $P_2 - P_1$ is termed side-on overpressure. If the shock reflects from a rigid surface, the pressure increases from P_1 to the reflected pressure P_5. The corresponding pressure increment $P_5 - P_1$ is termed face-on overpressure.

The changes of the thermodynamic properties of the gas can be determined using the Rankine-Hugoniot relations [1, 2, 4, 8]. The Rankine-Hugoniot relationships across a curved shock are the same as those for a plane shock, even for a very small radius of curvature. These relations can be written in a form that links the jump in pressure, density, temperature etc. immediately behind the shock front to the speed of the shock front, V_r usually expressed in form of the shock Mach number M_s:

$$M_s = \frac{V_r}{a_1},$$ (2.1)

where a_1 is the speed of sound in the gas ahead of the shock.

The normalized side-on overpressure immediately behind the shock, in terms of the shock Mach number, is given by

$$\frac{P_2 - P_1}{P_1} = \frac{2\gamma M_s^2 - 2\gamma}{\gamma + 1} = \Delta P_{21}$$ (2.2)

and the normalized reflected overpressure follows as [1, 4]

$$\frac{P_5 - P_1}{P_1} = 2\Delta P_{21} + \frac{(\gamma + 1)\Delta P_{21}^2}{(\gamma - 1)\Delta P_{21} + 2\gamma} = \Delta P_{51}$$ (2.3)

Equation (2.3) is derived under the assumption that the gas behind the reflected shock is brought to rest. This is not exactly fulfilled in the case of blast waves, where an expansion zone follows immediately behind the shock front causing a non-zero velocity of the flow when the wave reflects normally from a rigid wall. For the investigated range of distances and charge masses, however, this error appears to be negligible.

3.2 Overpressure data

Figure 3 shows a typical face-on overpressure-
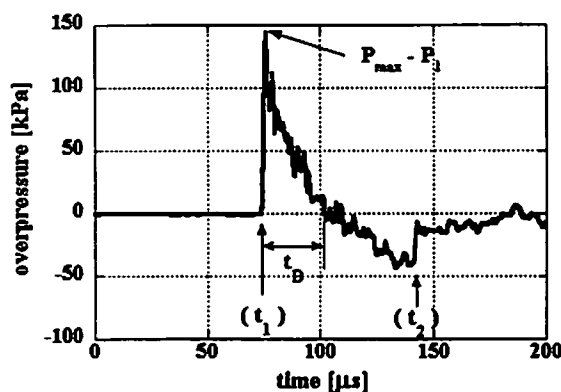
Fig. 3 Typical face-on overpressure-vs.-time trace for a blast wave generated by 5mg of silver azide at a distance of 45mm from the transducer

vs.-time trace of a blast wave, from which three essential blast wave parameters (face-on overpressure $P_{max} - P_1$, time of arrival t_1, duration of the positive pressure pulse t_p) can be obtained. Following the initial pressure jump at t_1 and the subsequent decay, at time t_2 a second but significantly smaller pressure jump is observed, caused by the so-called secondary shock, which is

a common (but usually weak and therefore mostly neglected) blast wave feature [1, 2]. The trace in Fig.3 represents the measured raw data. These traces have to be corrected and smoothened in order to account for imperfections of the measuring device, which result in an overshoot and ringing of the recorded signal. The correction procedure applied here corresponds to the one described in [4]. The time of arrival t_l is defined as the instant at which the overpressure reaches 10% of the recorded maximum value $P_{max} - P_l$ (see Fig.3). An exponential curve fit of the form $\Delta P = C_l \exp(-C_2 t)$ is made for the first half of the positive duration of the measured pressure pulse, i.e., for the time interval $t_D / 2 - t_l$. Figure 4 shows the corrected trace based on the measurement data of Fig.3. The corrected overpressure peak value $P_{corrected\ max}$ is obtained as the value of the derived curve fit for the instant t_l. In the given example, one obtains the following data:

$P_{max} - P_l$ (highest pressure value in Fig.3) = 143.6kPa,

$P_{corrected\ max} - P_l = 115.8 \pm 2$kPa,

$t_l = 74.85 \pm 0.25 \mu$s,

$t_D = 27.5 \mu$s.

From the complete series of experiments, an overpressure-vs.-range diagram of the type of Fig.7 can be established. The time of arrival data t_l from these tests were included in the x-t diagrams (Fig.6) and were seen to be in excellent agreement with the corresponding data from the independently carried out visualization.
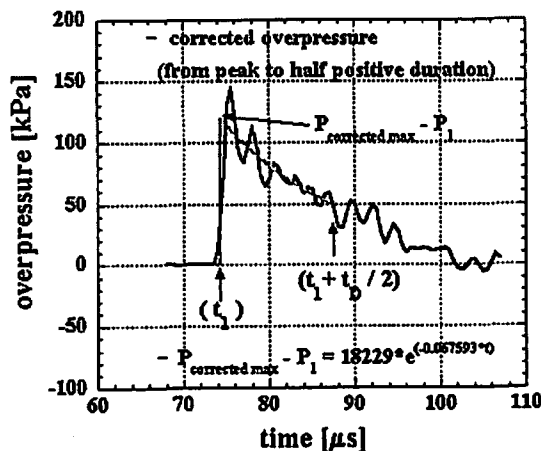
Fig. 4 Corrected trace based on the measurement of Fig.3

3.3 Visualization data
3.3.1 x-t diagram

From time-sequential photos of the blast wave obtained by the time-resolved schlieren method, such as the one shown in Fig.5, it is possible to measure with sufficient accuracy the loci of the discontinuities (primary shock wave, secondary shock wave, and the cloud of detonation products) and to establish an x-t diagram for all investigated charge masses (Fig.6). The size of the symbols representing the measurement points in Fig.6 is larger than the error bar associated with the uncertainties of the geometrical measurements. The decay in shock speed for the primary blast wave is more rapid for smaller charges than for large ones so that distinct x-t curves are established for each charge size. The propagation speed of the secondary shock, however, appears to be essentially constant for all investigated charge masses, at least within the accuracy of this measurement.

3.3.2 Overpressure from x-t data

Since the jump of the thermodynamic properties is intimately linked to the speed of the shock front, the time of arrival data can be used to independently obtain pressure values [2, 4]. Based on the x-t data from visualization and pressure measurements, an appropriate curve fit x = x (t) can be found for the data represented in Fig.6. The form of this fit is critical and a strictly monotonous function should be used [2]. Corresponding functions were determined for the x-t curve of all primary blast waves associated with each charge mass. Differentiation of these functions yields the charge-specific shock speed V_s from which according to the above relations the face-on overpressure can be determined. The results are presented together with the pressure measurements in Fig.7.

3.4 Face-on overpressure vs. scaled distance

The most common form of blast scaling is the "cube-root" scaling [9]. This states that at identical scaled distances self-similar blast waves are produced when two explosive charges of similar geometry and of the same explosive, but of different sizes, are detonated in the same atmosphere. It is
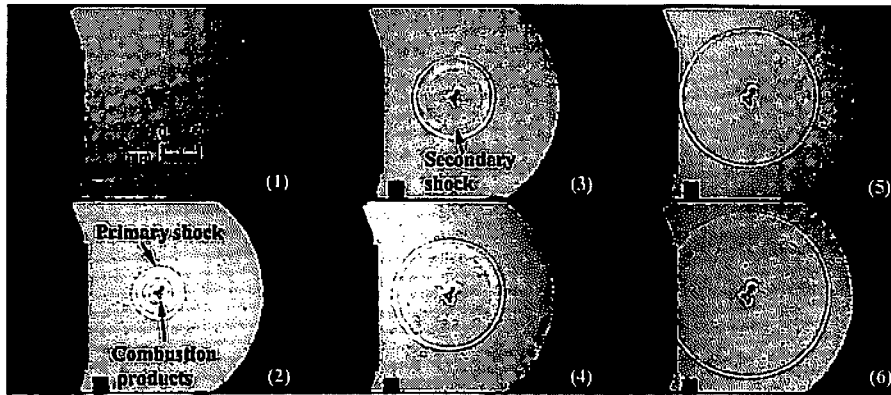
Fig. 5 Sequential photos of blast waves obtained with the time-resolved schlieren system. Instants of photography: (1) 5. 9μs, (2) 55. 9μs, (3) 105. 9μs, (4) 155. 9μs, (5) 205. 9μs, (6) 255. 9μs, after ignition of a 1mg silver azide charge.
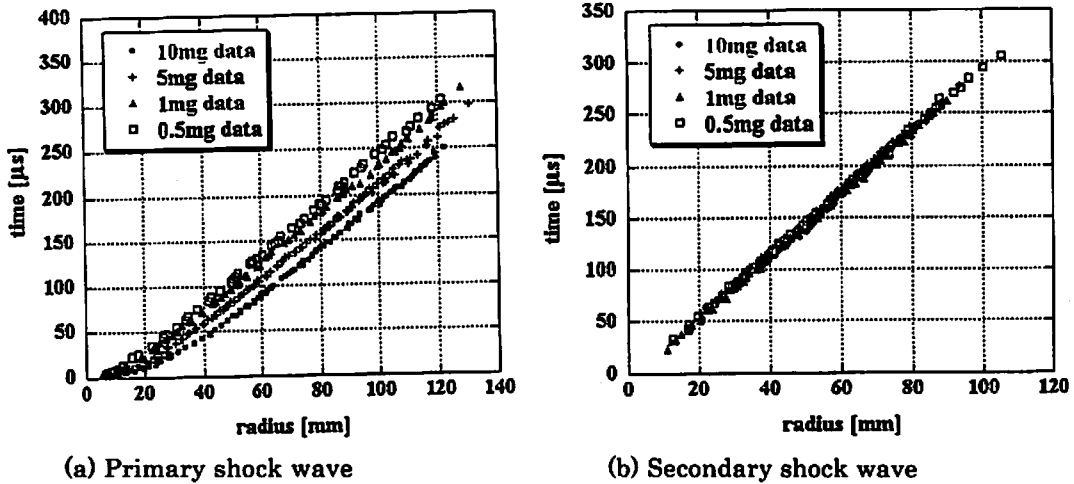
(a) Primary shock wave

(b) Secondary shock wave

Fig. 6 x-t diagram of primary and secondary shock waves for all investigated charge masses (10mg, 5mg, 1mg, 0.5mg)
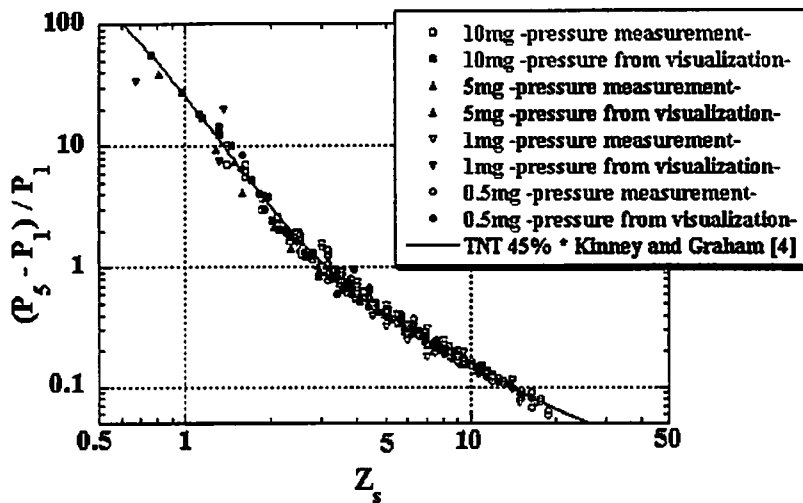
Fig. 7 Experimentally obtained face-on overpressure data vs. scaled distance in comparison with TNT reference data from [4] for an equivalence factor of 0.45.

customary to plot the blast property of interest (e.g., the overpressure) against the scaled distance Z_{HC} defined as

$$Z_{HC} = \frac{x}{W^{1/3}},\qquad (2.4)$$

where x is the distance from the center of the explosive source and W is the charge mass. This scaling law has been extended to account for differences in atmospheric conditions [10]. In this case, the previously defined overpressure ratios ΔP_{2t} or ΔP_{st} are plotted against the scaled distance

$$Z_S = \frac{x}{W^{1/3}} \times P_1^{1/3}.\qquad (2.5)$$

A great amount of reference data exists for TNT as 'standard' explosive. These data are normalized to standard atmospheric conditions ($P_0 = 101.25$ kPa, $T_0 = 288.15K$) and are available in tabulated form [1], as curve fits [4], or in databases [2]. In order to compare an explosive other than TNT with these reference data, W is to be interpreted as the equivalent TNT mass of the charge, i.e., the mass of TNT that would be necessary to generated a blast wave of the same characteristics as the one generated by the investigated charges (here: silver azide). This can be written as

$$W = W_{TNT} = \eta \times W_{silver azide}\qquad (2.6)$$

with η as the TNT equivalence factor. An explosive is seen to follow the scaling laws [9, 10] if all overpressure measurements for various charge masses and ambient conditions can be represented as one curve when plotted against the scaled distance Z_s given in (2.5). By comparing this curve with TNT reference data, an average equivalence factor η can be found by identifying the TNT reference curve closest to the measured data. Strictly speaking, η is a local value and will vary with distance from the charge, but for most engineering purposes it is sufficient to determine an average equivalence factor. Figure 7 shows the experimentally obtained face-on overpressure data vs. scaled distance in comparison with TNT reference data from [4] for an average equivalence factor of 0.45. The experimental data points, which represent about 1500 measurements obtained in more than 300 trials, lie reasonably close to the reference curve. Pressure and visualization data were found to be in very good agreement and give

virtually identical results. The value of η found in these experiments lies significantly below one value given in the literature [11], which was, however, determined for larger charges by the entirely different sand crush test method ($\eta_{lit} = 0.88$). Another reference ([12]) gives the equivalence factor of silver azide as $\eta = 0.4$, which is reasonably close to the result obtained here. The exact determination of η depends to a large extent on the blast property chosen for comparison and also on the selected set of reference data. Slight deviations from the value obtained here are possible if other blast properties (e.g., impulse or energy) and different reference sources (e.g., [1, 2]) are used. These differences will, however, be minor and would not account for the significant discrepancy between the value found here and the one given in [11].

4. Summary and conclusions

In order to characterize the properties of blast waves generated by milligram charges in free air, extensive flow visualization and pressure measurements were conducted. The results of these tests can be summarized as follows:

1. The propagation of primary and secondary blast waves for four different charge masses were mapped in corresponding x-t diagrams.
2. The blast waves generated by the investigated charges follow the scaling laws for the investigated range $1 < Zs < 20$ [m·atm$^{1/3}$ / kg$^{1/3}$].
3. Based on pressure and visualization records, the average TNT equivalence of silver azide was found to be approximately 0.45 (literature: AMC report 1977 [11]: $\eta = 0.88$ for sand crush test; Baker 1983 [12]: $\eta = 0.4$).
4. The propagation speed of the secondary shock wave appears to be essentially constant for all investigated charge masses (10 mg, 1 mg, 5 mg, 0.5 mg).

Other results, not described in detail here but in [13], indicate that

(a) In the early stage of the explosion, the blast wave is strongly distorted in the y-z plane, but

already highly symmetrical in the x-y plane.

(b) The distortion diminishes quickly but is not reproducible.

References

1) W.E.Baker: *Explosions in Air*, (University of Texas Press, Austin and London 1973).

2) J.M.Dewey: 'Expanding Spherical Shocks (Blast Waves)', In: Handbook of Shock Waves 2, eds.: G.Ben-Dor, O.Igra, and T.Elperin (Academic Press, Boston, San Diego 2001) pp.441-481.

3) J.M.Dewey: Shock waves from explosions, Chapter 16 in High Speed Photography and Photonics, ed: S.F.Ray (Focal Press, Oxford 1997), pp. 245-253.

4) G.F.Kinney and K.J.Graham: *Explosive Shocks in Air*, 2nd edn. (Springer-Verlag, New York 1985).

5) K.Ohashi, H.Kleine, and K.Takayama: Characteristics of blast waves generated by milligram charges, Proc ISSW 23 (2001), paper (#5985 CD proceedings).

6) T.Mizukaki: Quantitative visualization of shock waves. Doctoral thesis, Tohoku University, Sendai (2001) (in Japanese).

7) H.Kleine: 'Flow Visualization', In: Handbook of Shock Waves 1, eds.: G.Ben-Dor, O.Igra, and T.Elperin (Academic Press, Boston, San Diego 2001) pp.683-740.

8) H.W.Liepmann and A.Roshko: *Elements of Gasdynamics*, (John Wiley and Sons, New York 1957) .

9) B.Hopkinson: British Ordnance Board Minutes 13565 (1915).

10) P.G.Sachs: The Dependence of Blast on Ambient Pressure and Temperature, Aberdeen Proving Ground, Maryland, BRL Report No.466 (1944)

11) Army Material Command, AMC Pamphlet AMCP 706-177, January (1977).

12) W.E.Baker et al.: Explosive Hazards and Evaluation, Elsevier, Amsterdam, Netherlands (1983).

13) K.Ohashi: Experimental Characterization of Flow Fields Generated by Blast Waves and Supersonic Projectiles. Master thesis, Tohoku University, Sendai (2002).